1.3 NON-THERMOMETRIC EFFECTS ON MSU TROPOSPHERIC TEMPERATURES

Leslie Litten, John R. Christy and Roy W. Spencer
University of Alabama in Huntsville, Huntsville, Alabama USA

1. INTRODUCTION

The University of Alabama in Huntsville (UAH) pioneered the use of microwave brightness temperatures for the purpose of monitoring global, deep-layer temperature changes over decadal scales. Microwave radiometers detect emissions near the 60 GHz oxygen absorption band where oxygen behaves as a blackbody. Since atmospheric oxygen is well-mixed, its temperature is representative of the temperature of the atmosphere.

However, there have been concerns about the effects of physical processes which confound the oxygen brightness temperature by contributing to or somehow affecting emissions receive at the radiometer (Spencer et al. 1990). Speculation has been made that these effects may contaminate the atmospheric temperature signal (e.g. NRC 2000.) This study specifically addresses several sources of potential temperature contamination using several independent sources of radiometric (and other) data which are able to quantify such effects. In particular we examined the effects of changes in surface emissivity (land and snow), sea ice, ocean roughening, cloud liquid water and precipitable water.

2. BACKGROUND

The tropospheric temperatures generated by UAH portray the bulk atmospheric temperature of two broad layers. Microwave Sounding Unit (MSU) channel 2 measures emission from the entire atmosphere with a peak in the mid troposphere ($T_{Mid\text{-}Trop}$). A second product uses a linear combination of the slightly different weighting functions of MSU2 between nadir views and limb views, to eliminate the stratospheric portion of $T_{Mid\text{-}Trop}$ to produce a lower tropospheric layer temperature ($T_{Low\text{-}Trop}$).

Though most of the emissions detected by the MSU2 radiometer originate from atmospheric oxygen, other sources contribute. The largest secondary source of emissions is the surface, for $T_{Mid\text{-}Trop}$ about 5% over oceans and 10% over land; the difference is due to the fact the emissivity of the ocean skin is only about 0.5 while that of land skin is 0.9. The contribution of surface emissions is magnified in $T_{Low\text{-}Trop}$, being about double that of $T_{Mid\text{-}Trop}$.

The ocean's surface emissivity is low, producing a "cold" background to the atmosphere. However, when the surface is roughened and foam appears, the emissivity increases causing the surface brightness temperature to increase, which is observed as a warming of the total brightness temperature. Thus, ocean roughening can cause brightness temperature changes without a true change in temperature (Wisler and Hollinger 1977). Sea ice has a greater emissivity than the ocean skin (between that of water and land), so that an increase in emissions (and brightness temperature) occurs in the presence of sea ice (Cavalieri et al. 1985).

Land generally has an emissivity of 0.90-0.96. However when large precipitation events occur, the emissivity will change. If the land becomes wholly or partially covered in water, the surface emissivity will drop as will the observed brightness temperature (Basist et al. 1998). Additionally, the skin surface of snow has a lower emissivity than 0.9. Thus changes in the water or snow covering of land will be viewed as changes in brightness temperature even thought the atmospheric temperature may not have changed.

In the atmosphere itself, water vapor emits microwave radiation. Over oceans, increased water vapor, which is essentially always at low, warm levels, will act to increase the emissions

Corresponding Author address: John R. Christy, ESSC/NSSTC, University of Alabama in Huntsville, Huntsville AL 35899. christy@nsstc.uah.edu

detected by satellite. Over land, the background is warm or "bright" due to land emissivities. In this case additional water vapor will emit at atmospheric temperatures which are cooler than the background land, and thus induce a spurious cooling effect on the microwave observation.

Cloud droplets will emit near the blackbody temperature, so against the cold ocean background, low clouds will appear as a warming influence because they emit at the relatively warm temperatures of the lower atmosphere. Mid-level clouds over the ocean are at colder atmospheric altitudes and thus can induce a colder temperature than seen in the ocean skin background. So, over the ocean, low clouds tend to cause a spurious warming to the observed brightness temperature while mid-level water clouds induce a cooling. Ice clouds have little influence on the microwave emissions.

The situation over land is a bit different. The background surface appears warm or "bright" due to the high emissivity. A low cloud will typically emit at a lower temperature than the land skin, so that low clouds will lead to a spurious cooling observation for that portion of the signal with which they interfere. Mid-level water clouds, as with the ocean, will lead to a cooling of the observed brightness temperature.

3. DATA AND METHOD

Several data products derived from other satellite sensors provide the information necessary to quantify the non-thermometric effects discussed thus far. The Special Sensor Microwave (SSM/I) on board DMSP satellites monitors several frequencies. Table 1 lists (a) the various products used in this study, (b) the radiometric source of needed to produce the dataset, (c) the range of the product over the earth for 1988-2001 at the gridpoint level, (d) the atmospheric profile used and (e) the estimated impact on the $T_{Mid\text{-}Trop}$ per change in the variable identified.

Most data were provided by Remote Sensing Systems of San Rafael CA (RSS) including ocean winds, cloud liquid water and precipitable water (Wentz 1997). Calculations of sea ice were generated by two groups, the NASA Team and Bristol (Cavalieri 1996, Smith 1996). Surface emissivities over land were calculated as a part of this study using the method and data provided by A. Basist (Williams et al. 2000). ISCCP generates cloud liquid water and precipitable water (Schiffer et al. 1985). Thus, there are many permutations of these datasets which when combined provide estimates of the total non-thermometric impact on the microwave brightness temperature.

4. RESULTS

4.1 Surface emissivity

Fields of each quantity were generated by month so that regional variations could be examined as well as a calculation of the global mean effect of these various non-thermometric issues. In Fig. 1 is displayed the variation of surface emissivity due to the combination of all of the surface factors on the land and ocean for the 13 Januaries studied. Note that the variations are calculated by grid point, so that these do not represent a particular month, but have grids representing many Januaries. The net effect on the $T_{Mid\text{-}Trop}$ temperature is shown in Fig. 2 for two climate extremes, the cool period following the eruption of Mt. Pinatubo (Jul-Dec 1992) and the warm period of the major ENSO event (Jan-Jun 1998). What is evident is that the impact on the brightness temperature is extremely small for six-month averages (few hundredths of a degree at the grid point level.)

4.2 Cloud liquid water

There are two datasets utilized here. RSS provides a single, microwave-based estimate of cloud liquid water for the entire atmospheric column, but only over oceans (because the measurment requires a cold background). ISCCP produces a dataset of low and mid-cloud amounts, over land and ocean, and is thus able to distinguish the two opposite effects of cloud water at different elevations over oceans. However, the ISCCP dataset appears more unstable, with large excursions from the mean that are not indicated by RSS.

The results are quantitatively different. Based on RSS ocean data, there are only very small changes from month to month the anomalies of which impact the global $T_{Mid\text{-}Trop}$ by no more than 0.02 K in any given month. ISCCP values are also generally small except for significant excursions of 0.06 °C in early 1994 when cloud data show a sharp decrease in mid-level cloudiness for a few months. Otherwise, ISCCP values are also in the range of 0.02 K as globally-averaged monthly impacts on $T_{Mid\text{-}Trop}$.

4.3 Precipitable water

RSS and ISCCP provide estimates of precipitable water, again with RSS being ocean only. Local variations in PW for 6-month averages show impacts on the tropospheric brightness temperature of < 0.05 K. Globally-averaged monthly variations of RSS impart much less than 0.01 K deviations to the brightness temperature. Global-mean, ocean-only ISCCP variations rise to 0.02 K in 1998-2000, but these are thought to be problematic.

5. SUMMARY AND CONCLUSIONS

When all contributions to the brightness temperature are included, we find that the non-thermometric contribution is very small. In Fig. 3 we show the effects on the local TMid-Trop between the two most extreme 6-month periods. Locally, differences on the order of 0.2 K can be found. Globally, the differences are minuscule. In Fig. 4 we show the impact of the non-thermometric contributions compared with the currently reported UAH $T_{Mid\text{-}Trop}$ and $T_{Low\text{-}Trop}$ using the RSS values for cloud-liquid water and precipitable water. We see that if these contributions are accurate, the effect on the time series is no more than 0.01 C/decade, well within the reported precision of the UAH datasets (±0.05 K/decade, Christy et al. 2003). Thus, these non-thermometric effects are negligible relative to the trends of the past two decades.

6. REFERENCES

Basist, Norman C. Grody, Thomas C. Peterson, Claude N. Williams, 1998: Using the Special Sensor Microwave/Imager to Monitor Land Surface Temperatures, Wetness, and Snow Cover. Journal of Applied Meteorology: Vol. 37, No. 9, pp. 888-911.

Cavalieri, D., 1996: NASA Team Sea Ice Algorithm. http://nsidc.org/data/docs/daac/nasateam/index.html

--, and H.J. Zwally, 1985: Satellite observations of sea ice. Advanced Space Research 5:247- 255.

Christy, J.R., R. W. Spencer, W. B. Norris, D. Braswell and D.E.Parker 2003: Error estimates of Version 5.0 of MSU/AMSU Bulk Atmospheric Temperatures. J. Atmos. Oc. Tech. 20, 613-629.

NRC 2000; Reconciling Observations of Global Temperature Change. National Academy Press.85 pp.

Schiffer, R.A., and Rossow, W.B., 1985: ISCCP Global Radiance Data Set: A New Resource for Climate Research. *Bull. Amer. Meteor. Soc.*, **66**, 1498-1505. Read abstract and download PDF document (9pp).

Smith, D.M., 1996: Extraction of winter total sea-ice concentration in the Greenland and Barents Seas from SSM/I data. *International Journal of Remote Sensing* 17(33): 2625-2646.

Spencer, R. W., and J. R. Christy, 1990: Precise monitoring of global temperature trends from satellites. Science, 247, 1558-1562.

Spencer, R. W. , J. R. Christy and N. C. Grody, 1990: Global atmospheric temperature monitoring with satellite microwave measurements: Method and results 1979-1985. *J. Climate*, **3**, 1111-1128.

Wentz, 1997. A well calibrated ocean algorithm for special sensor microwave/imager. Journal of Geophysical Research 102(C4):8703-8718.

Williams, Claude N., Alan Basist, Thomas C. Peterson, Norman Grody, 2000: Calibration and Verification of Land Surface Temperature Anomalies Derived from the SSM/I. Bulletin of the American Meteorological Society: Vol. 81, No. 9, pp. 2141-2156.

Wisler, M. M. and J. P. Hollinger, 1977: Estimation of marine environmental parameters using microwave radiometric remote sensing systems. N.R.L. Memo. Rept. 3661, pp 27.

Table 1 Listing of quantities examined for their imprint on the tropospheric brightness temperature as measured by microwave emissions near the 60 GHz absorption band. Frequencies listed are observed on DMSP satellites.

Quantity	Frequencies Used (GHz)	Range (emissivity or water content)	Atmosphere	Estimated Impact on MT
Land Surface Temp	**37V, 37H, 85V, 85H**	**.62 - .96**		**1K/emiss □**
NASA Team Sea Ice	**19V, 19H, 37V**	**.62 - .96**		**1K/emiss □**
Bristol Sea Ice	**19V, 37V, 37H**	**.62 - .96**		**1K/emiss □**
Ocean Emissivity	**19V, 19H, 22V, 22H, 37V, 37H**	**.48 - .56**		**0.01K-s/m**
Water Vapor (land)	**19V, 19H, 22V, 22H, 37V, 37H**	**0 – 70 mm**	**Polar**	**0K/mm**
Water Vapor (land)	**19V, 19H, 22V, 22H, 37V, 37H**	**0 – 70 mm**	**Std**	**-1K/mm**
Water Vapor (land)	**19V, 19H, 22V, 22H, 37V, 37H**	**0 – 70 mm**	**Trop**	**-1K/mm**
Water Vapor (ocean)	**19V, 19H, 22V, 22H, 37V, 37H**	**0 – 70 mm**	**Polar**	**1K/mm**
Water Vapor (ocean)	**19V, 19H, 22V, 22H, 37V, 37H**	**0 – 70 mm**	**Std**	**1K/mm**
Water Vapor (ocean)	**19V, 19H, 22V, 22H, 37V, 37H**	**0 – 70 mm**	**Trop**	**1K/mm**
Cloud Liquid Water (land)	**19V, 19H, 22V, 22H, 37V, 37H**	**0 – 2 mm**	**Low**	**-1.3K/mm**
Cloud Liquid Water (land)	**19V, 19H, 22V, 22H, 37V, 37H**	**0 – 2 mm**	**Mid**	**-3K/mm**
Cloud Liquid Water (ocean)	**19V, 19H, 22V, 22H, 37V, 37H**	**0 – 2 mm**	**Low**	**2K/mm**
Cloud Liquid Water (ocean)	**19V, 19H, 22V, 22H, 37V, 37H**	**0 – 2 mm**	**Mid**	**-1.7K/mm**

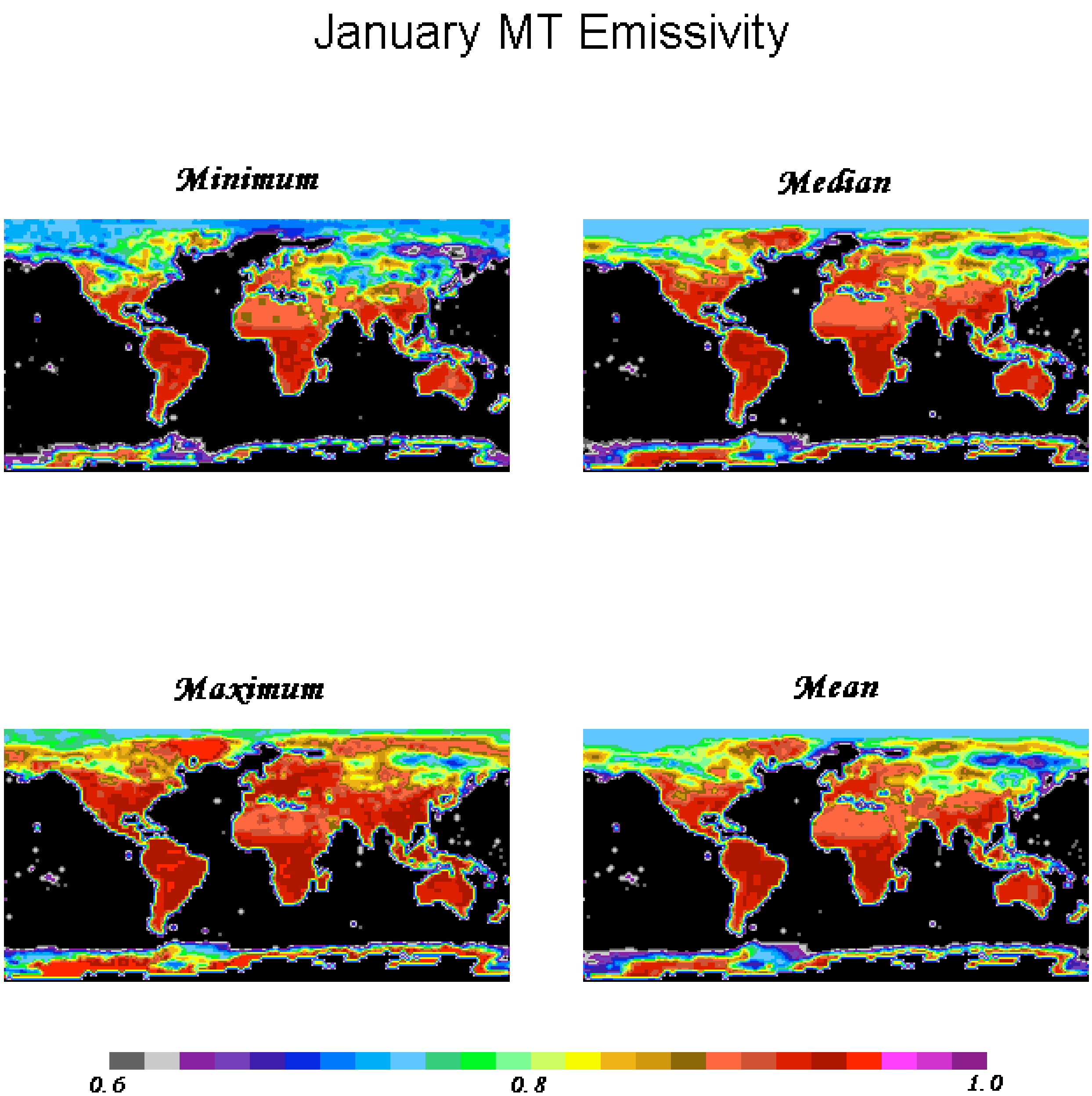

Figure 1

Figure 1. Local variation of emissivity due to land and sea ice variations. Each grid is an independent calculation for each quantity (i.e. these do not represent actual maps of a particular month.)

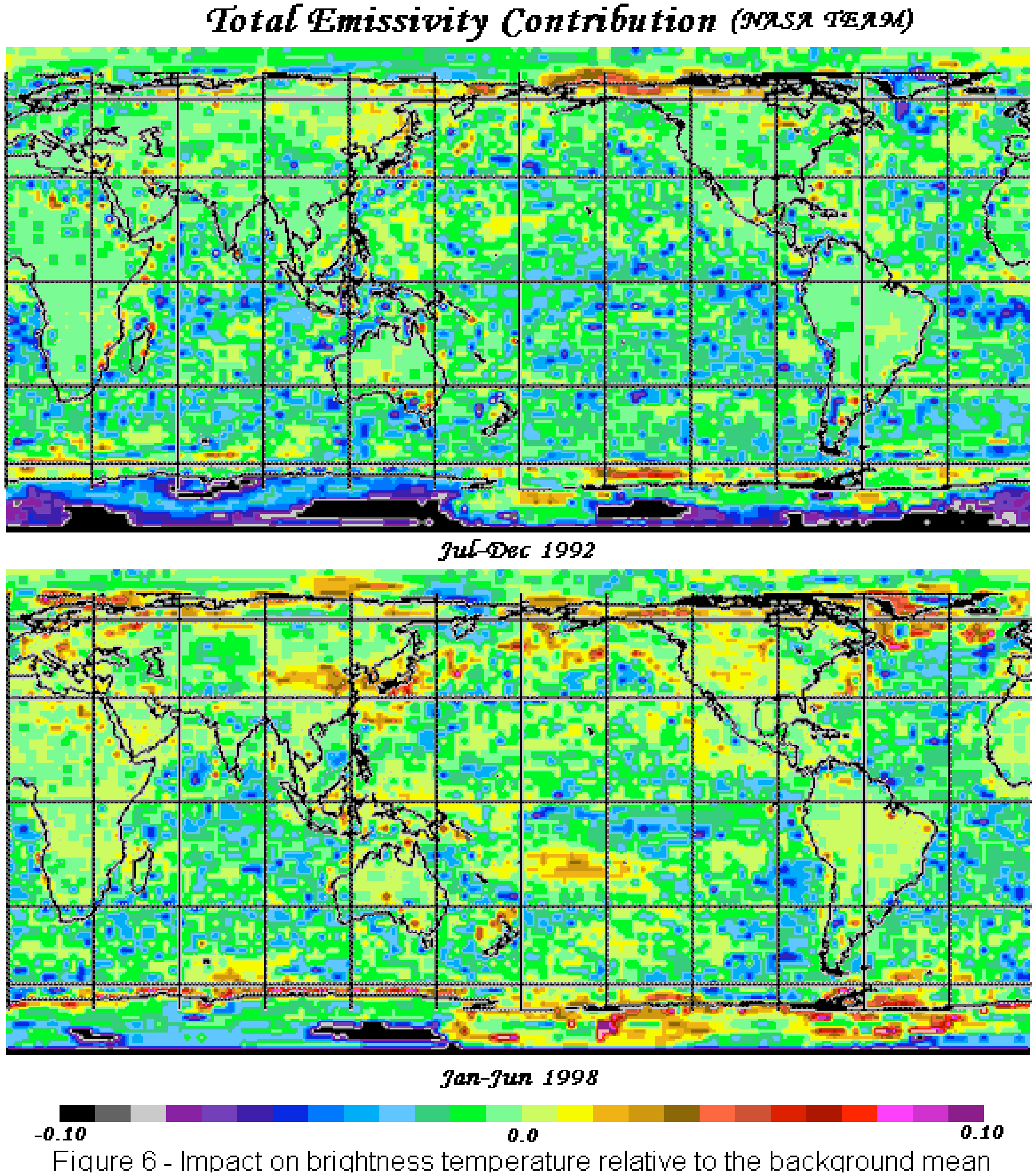

Figure 2 Impact on $T_{Mid\text{-}Trop}$ by sum of the surface emissivity variations for two 6-month periods, Jul-Dec 1992 (top) and Jan-Jun 1998 (bottom).

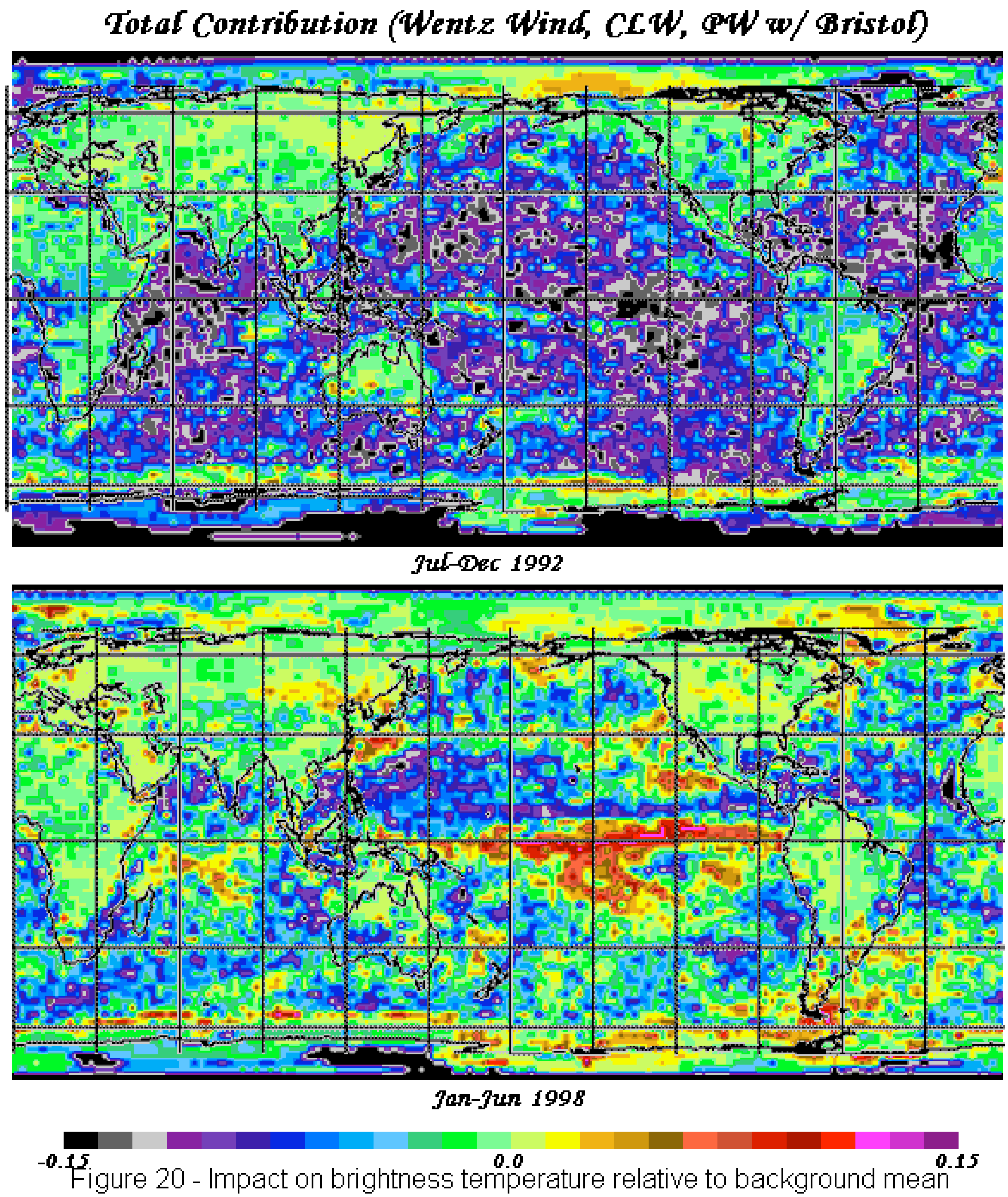

Figure 3. Impact on local $T_{Mid\text{-}Trop}$ temperature by the sum of all non-thermometric effects discussed in this paper for two 6-month averages, top Jul-Dec 1992 and Jan – Jun 1998.

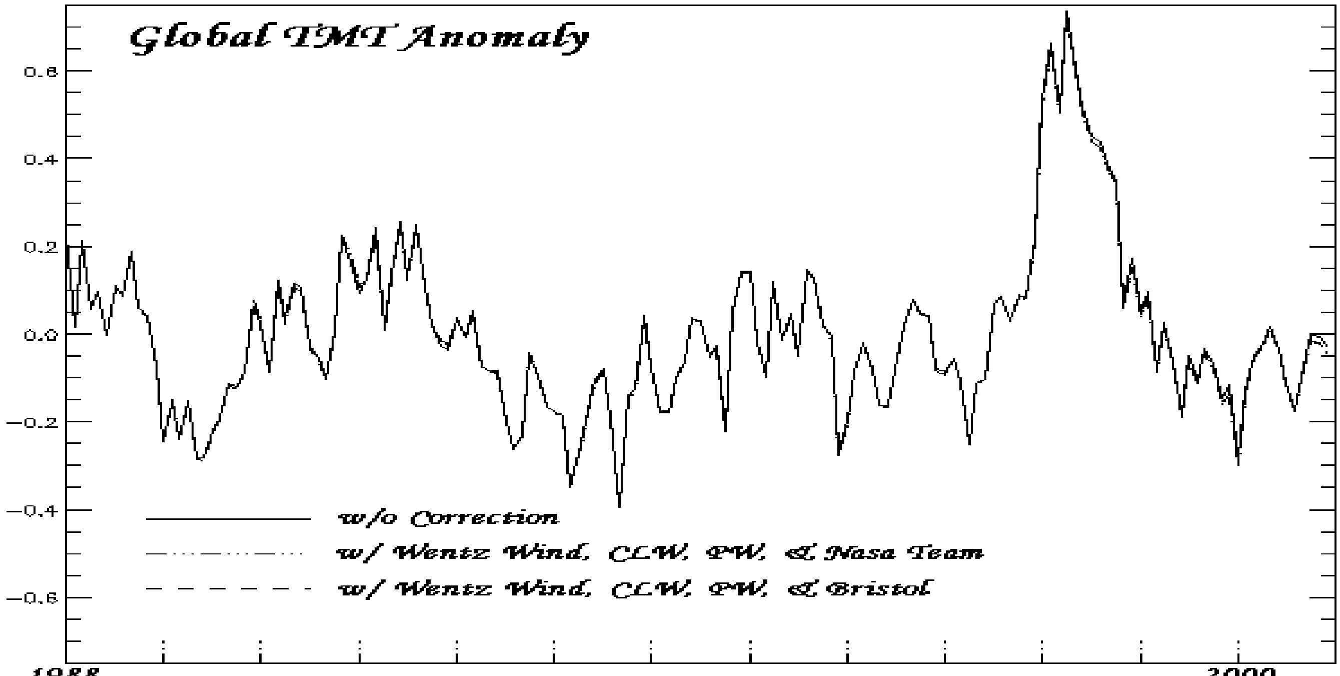

Figure 27

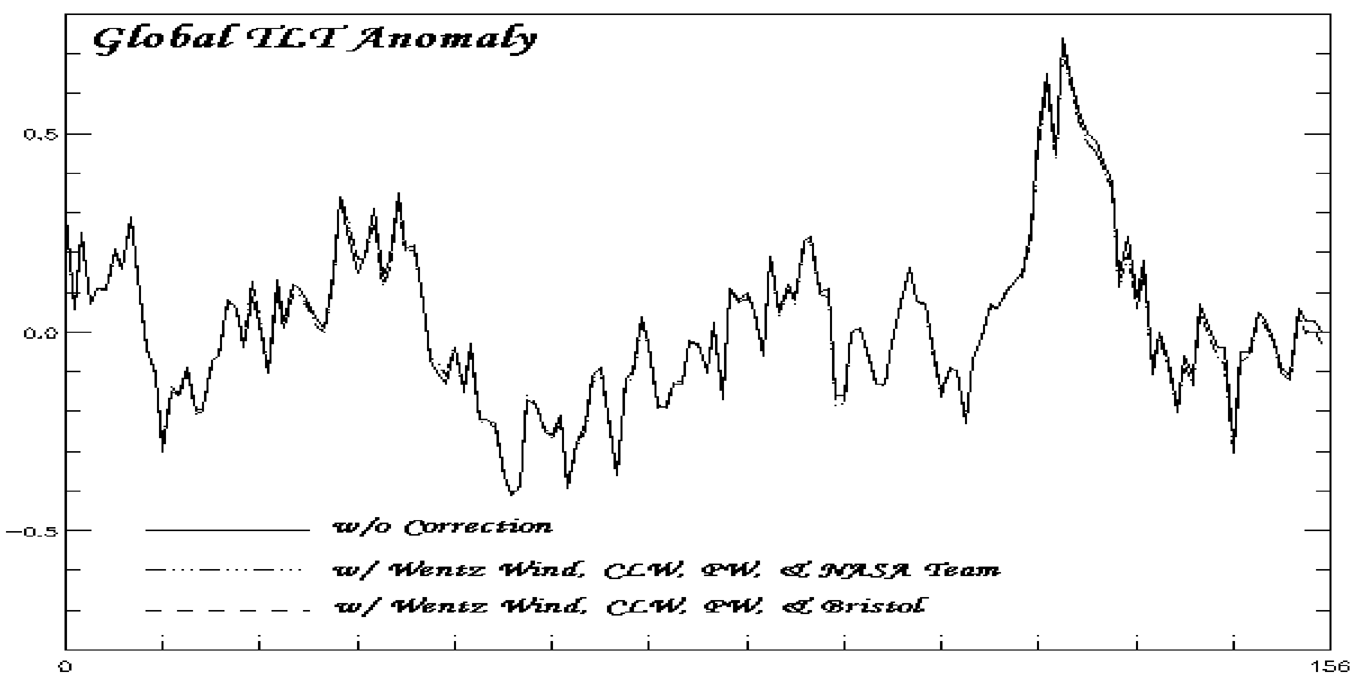

Figure 30

Figure 4a (Top) Time series of $T_{Mid\text{-}Trop}$ (MSU channel 2) w/o non-thermometric corrections (solid line) and with (dashed). Figure 4b (Bottom) as above but for $T_{Low\text{-}Trop}$ (MSU channel 2 retrieval.)